AFRL-AFOSR-VA-TR-2019-0348

Microcavity polaritonics based on van der Waals heterostructures

Anthony Vamivakas
UNIVERSITY OF ROCHESTER

03/07/2019
Final Report

Air Force Research Laboratory
AF Office Of Scientific Research (AFOSR)/ RTA1
Arlington, Virginia 22203
Air Force Materiel Command

REPORT DOCUMENTATION PAGE

Form Approved
OMB No. 0704-0188

1. REPORT DATE *(DD-MM-YYYY)*	2. REPORT TYPE	3. DATES COVERED *(From - To)*
15-11-2019	Final Performance	01 Nov 2015 to 31 Oct 2018

4. TITLE AND SUBTITLE
Microcavity polaritonics based on van der Waals heterostructures

5a. CONTRACT NUMBER

5b. GRANT NUMBER
FA9550-16-1-0020

5c. PROGRAM ELEMENT NUMBER
61102F

6. AUTHOR(S)
Anthony Vamivakas

5d. PROJECT NUMBER

5e. TASK NUMBER

5f. WORK UNIT NUMBER

7. PERFORMING ORGANIZATION NAME(S) AND ADDRESS(ES)
UNIVERSITY OF ROCHESTER
910 GENESEE ST STE 200
ROCHESTER, NY 14611-3847 US

8. PERFORMING ORGANIZATION REPORT NUMBER

9. SPONSORING/MONITORING AGENCY NAME(S) AND ADDRESS(ES)
AF Office of Scientific Research
875 N. Randolph St. Room 3112
Arlington, VA 22203

10. SPONSOR/MONITOR'S ACRONYM(S)
AFRL/AFOSR RTA1

11. SPONSOR/MONITOR'S REPORT NUMBER(S)
AFRL-AFOSR-VA-TR-2019-0348

12. DISTRIBUTION/AVAILABILITY STATEMENT
A DISTRIBUTION UNLIMITED: PB Public Release

13. SUPPLEMENTARY NOTES

14. ABSTRACT
The research of our effort were to investigate a novel platform to realize semiconductor microcavity polaritons. In contrast to all previous work, van der Waals heterostructures, based on two-dimensional atomically thin materials, served as the matter system that is coupled to a semiconductor optical cavity. Atomically thin semiconductors support both quantum-dot (ie localized, 0D) and two-dimensional (2D) extended excitons that can be seamlessly integrated with nanophotonic devices. The large binding energy exhibited by the 2d excitons in two-dimensional semiconductors allowed for stable room temperature exciton formation and the realization of novel polaritonic based optoelectronic devices. In this research program, we fabricated and characterized semiconductor optical cavities suitable to couple with excitons in atomically thin semiconductors and their van der Waal's heterostructures. We specifically observed the formation of charged exciton (trion) cavity polaritons. These trion-polaritons exhibit anomalous dispersion and should allow for the formation of interesting quantum matter states. We also observed indications of room temperature quantum coherence in the form of coherent valley polaritons.

15. SUBJECT TERMS
van der Waals heterostructures, polaritons, two-dimensional materials, 2D materials, light-matter interaction, excitons

16. SECURITY CLASSIFICATION OF:			17. LIMITATION OF ABSTRACT	18. NUMBER OF PAGES	19a. NAME OF RESPONSIBLE PERSON
a. REPORT	b. ABSTRACT	c. THIS PAGE			POMRENKE, GERNOT
Unclassified	Unclassified	Unclassified	UU		

				19b. TELEPHONE NUMBER *(Include area code)* 703-696-8426

DISTRIBUTION A: Distribution approved for public release.

Final Report: Microcavity polaritonics based on van der Waals heterostructures

Statement of Objectives

Main Objectives: The research plans detailed in this proposal explored a novel platform to realize semiconductor microcavity polaritons. In contrast to all previous work, van der Waals heterostructures, based on two-dimensional atomically thin materials, served as the matter system that is coupled to a semiconductor optical cavity. Atomically thin semiconductors support both quantum-dot (ie localized, 0D) and two-dimensional (2D) extended excitons that can be seamlessly integrated with nanophotonic devices. The large binding energy exhibited by the 2d excitons in two-dimensional semiconductors enables stable room temperature exciton formation and the realization of novel polaritonic based optoelectronic devices. In the research program, we fabricated and characterized semiconductor optical cavities suitable to couple with excitons in atomically thin semiconductors and their van der Waal's heterostructures. Van der Waals heterostructures including doped tungsten diselenide, doped molybdenum disulfide, graphene and hexagonal boron nitride will enable pn-junction formation for electrical injection and electrical control of 2D excitons via the quantum confined Stark effect. Finally, a device, based on a van der Waals heterostructure, that supports room temperature microcavity polariton formation and electrical injection will be realized such that this unique platform will enable novel light emitting diode and lasing modalities.

Novelty and Context: New ideas continuously emerge to address fundamental and technological challenges at the intersection of materials science, nano-optics, condensed matter physics, and nanotechnology. *Particularly exciting is to engineer nanophotonic devices that support confined exitonic and optical modes that result in* ***enhanced light-matter interaction***. Microcavity polaritons, hybrid excitations of material excitons and optical cavity modes, are a prototypical example of devices that support such controlled interactions. Since pioneering experiments in the early 1990's, microcavity polaritons have been extensively studied. It was only last year that the efforts of this research culminated with the demonstration of an electrically injected polariton laser based on III-V materials, albeit at low temperatures. In parallel, during the last decade, it has been realized that atomically thin materials, and their heterostructures, exhibit unique optical and electronic properties ***that can be engineered*** to provide the basis for a new generation of optoelectronics devices. Completely unexplored in this regard are cavity polaritons based on the excitons in these unique materials. Particularly attractive is the large exciton binding energy that will enable room temperature microcavity polariton formation and potentially threshhold-less lasers. Equally exciting are devices that leverage the unique properties of the two-dimensional material's electronic structure such as the spin or valley degree-of-freedom. The envisioned microcavity polariton devices – spin and/or valley LEDs and lasers –would find application in both spintronics and the emerging area of valleytronics.

Summary of project milestones: The ambitious goals and milestones of this proposal were:

- Demonstrate cavity polaritons based on van der Waal (vdW) heterostructure excitons
- Quantum confined Stark effect control of a vdW heterostructure's excitons
- Electrically pumped light emission from vdW heterostructure based cavity polaritons
- Nano-polaritonic modulators based on neutral and charged cavity polaritons

2. Summary of results from AFOSR FA9550-16-1-0020

Results from AFOSR FA9550-16-1-0020: The previous program resulted in 10 publications the most notable being the discovery of anomalous dispersing trion polaritons reported in Nature Physics[1]1. The previous work received substantial publicity in the popular science media with articles on Newsweek (http://www.newsweek.com/particle-physics-mind-bending-negative-mass-device-lasers-778495) and Futurity (http://www.futurity.org/negative-mass-particles-1646382-2/) to name just a few. There were also more than 20 invited colloquia, seminars and conference talks resulting from this program.

Here is a list of the publications resulting directly from this program:

[1] C. Chakraborty, A. Mukherjee and A. N. Vamivakas Electrically tunable valley polarization and valley coherence in monolayer WSe2 embedded in a van der Waals heterostructure, Optical Materials Express, in press (2019).

[2] C. Chakraborty, N. Jungwirth, G. Fuchs and A. N. Vamivakas, Electrical manipulation of the fine-structure splitting of WSe2 quantum emitters, Physical Review B, in press (2019).

[3] K. Konthasinghe, C. Chakraborty, N. Mathur, L. Qiu, A. Mukherjee, G. Fuchs and A. N. Vamivakas, Resonance fluorescence from a hexagonal boron nitride quantum emitter, under review (2018).

[4] M. Atature, D. Englund, A. N. Vamivakas, and J. Wratchrup, Material platforms for spin-based photonic quantum technologies, Nature Reviews Materials (2018). (in press)

[5] C. Chakraborty, L. Qiu, K. Konthasinghe, A. Mukherjee, S. Dhara, and A. N. Vamivakas, 3D Localized Trions in Monolayer WSe2 in a Charge Tunable van der Waals Heterostructure, Nano Letters (2018) in press.

[6] 2. S. Dhara, C. Chakraborty, L. Qiu, K. Goodfellow, T. Oloughlin, G. Wicks, and A. N. Vamivakas, Anomalous dispersion of microcavity trion-polaritons, Nature Physics 14, 130–133 (2018).

[7] C. Chakraborty, K. Goodfellow, S. Dhara and A. N. Vamivakas, Quantum confined Stark effect of quantum dots in van Der Waals heterostructures, Nano Letters 17 (4), 2253-2258 (2017).

[8] C. Chakraborty, K. M. Goodfellow, and A. N. Vamivakas, Localized emission from defects in MoSe2 layers, Optical Materials Express 6, 2081 (2016).

[9] L. Kinnischtzke, K. M Goodfellow, C.Chakraborty, Yi-M. Lai, S. Fält, W. Wegscheider, A. Badolato, and A. N. Vamivakas, Graphene mediated Stark shifting of quantum dot energy levels, Applied Physics Letters, 108, 211905, (2016).

[10] T. Malhotra, R.-C. Ge, M. Kamandar Dezfouli, A. Badolato, A. N. Vamivakas, and S. Hughes, Quasinormal mode theory and design of on-chip single photon emitters in photonic crystal coupled-cavity waveguidese, Optics Express 24, 13574 (2016).

Awards during AFOSR FA9550-16-1-0020: During the course of this program, the PI was awarded the **NSF CAREER Award (2016)**, selected as the University of Rochester, **Hajim Engineer of the Year Recipient (2016)**, selected as the **Leonard Mandel Faculty Fellow in Quantum Optics (2016)**, elected an **Optical Society of America Fellow (2018)** and selected as finalist for **Rochester Young Engineer of the Year (2018)**.

2. Outcomes of the program

The last two years has witnessed lots of activity studying polaritons formed from 2D materials. The PI's group has been at the forefront of this, making tremendous progress on realizing cavity polaritons with monolayer tungsten diselenide (WSe_2), monolayer molybdenum diselenide ($MoSe_2$) and a heterostructure of the two materials as a pathway to cavity polaritons with van der Waals heterostructure-excitons. Figure 1a illustrates the first generation of devices made in the PI's lab. They consist of planar distributed Bragg mirrors (DBR) made from SiO_2/Ta_2O_5 (the index is 1.4 and 2.1 at the $MoSe_2$ exciton wavelength of 770 nm). Single layer WSe_2, single layer $MoSe_2$ and a heterostructure of the two materials have been embedded in the cavity formed by the DBR. As previously mentioned, when light interacts with cavity-confined excitons, the cavity photons and excitons hybridize to form composite excitations known as cavity-polaritons. Figure 1b presents simulations of the dispersion relation of both the uncoupled exciton (dispersion-less) and the dispersive cavity photon mode. Also shown are the upper and lower polariton branches that form when the two excitations are hybridized assuming the cavity is red detuned from the exciton by 10 meV. The strength of the splitting is determined by the pronounced coupling between the exciton and cavity photon. Observation of this dispersion relation is a critical first step to realizing optoelectronic devices based on polaritons as well as to exploring Bose and Fermi condensation in the solid-state. The reason for the three different devices is as follows. Single layer WSe_2 and $MoSe_2$ both exhibit large binding energies and pronounced neutral and charged exciton (trion) peaks. We anticipate coupling these materials will result polariton formation from excitons and trions. The vertical heterostructure can form indirect exciton cavity polaritons, whereby its longer lifetimes will promote condensation formation.

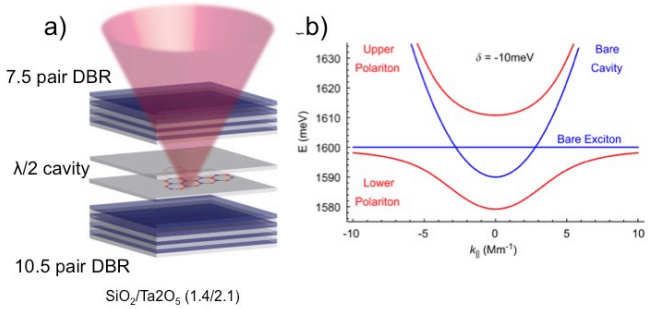

Figure 1. TMDC microcavity polaritons. a) Illustration of fabricated planar microcavity containing a single layer of atomically thin semiconductor. **b)** Formation of microcavity polaritons when the cavity and exciton are slightly detuned. Bothe the uncoupled and coupled dispersion relations are illustrated. This should be compared with the data in Fig. 6.

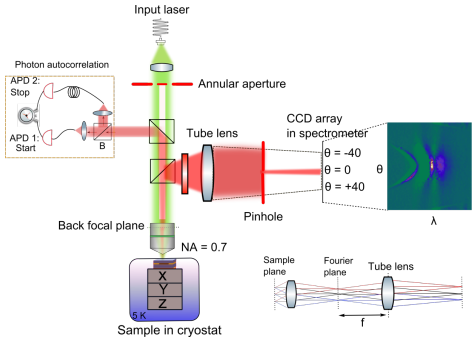

Figure 2. Angle resolved reflectance/ and photoluminescence setup. Sketch of the experimental setup constructed in the PI's lab capable of measuring the microcavity polariton dispersion relation. It is based on imaging the collection objective back focal plane onto the spectrometer CCD array.

To measure this novel dispersion relation, as part of AFOSR FA9550-16-1-0020, we built an angle resolved reflectance and photoluminescence spectroscopy instrument; see Fig. 2. The optical system uses a high numerical aperture objective lens (numerical aperture = 0.7) that has a collection angle of $\sim \pm 40°$ which covers most of the relevant wave vector range in the energy dispersion. Imaging the objective Fourier plane through a spectrometer onto a CCD allows us to get a single shot measurement of the entire polariton dispersion (right side,

Fig. 2). Figure 3 shows the angle resolved photoluminescence spectrum from the device illustrated in Fig. 1a. Also shown are the angle resolved uncoupled exciton (energy ~1.65 eV) and trion (energy ~1.62 eV) PL. These lines are flat and do not exhibit any dispersion. In this sample, the cavity detuning is ~ 5 meV from the exciton resonance at zero in plane momentum. As is evidenced from the presented data, hybridization between the neutral exciton and the cavity photon into upper and lower polariton branches occurs in this device (see Fig. 1b for comparison). The upper polariton branch (UPB) is the most energetic dispersion curve and the middle feature in the dispersion relation we refer to as the middle polariton branch (MPB) that forms with the $MoSe_2$ neutral exciton. For comparison, plotted in Fig. 3b are the momentum resolved emission spectrum. The data in Fig. 6a clearly demonstrates the formation of cavity polaritons.

In contrast to the simulation results of Fig. 1b, there is a third dispersion curve observed in our data. This new spectral feature arises from the charged $MoSe_2$ exciton (the trion) hybridizing with the cavity photon mode. The polariton branch emerging from trion hybridization exhibits a anomalous negative dispersion relation (lower polariton branch; LPB). The interesting physics associated with this branch stems from its extra electron. In contrast to the MPB, that are bosonic particles, the LPB particles are of Fermionic character. We understand the negative dispersion as resulting from an electron mediated attractive interaction between the exciton-polariton branch and the trion-polariton that overwhelms the weak trion cavity repulsion. The origin of such an attractive interaction may be understood in terms of exchange of an electron between a neutral exciton and the negatively charged trion thus delocalizing the trion's electron. Specifically, strong coupling of the exciton resonance with the cavity photon reduces the exciton-polariton's detuning with the trion resonance near $k_{||}$=0. Therefore, the gap between the exciton-polariton and the trion-polariton branch is a function of the in-plane wavevector resulting in a $k_{||}$ dependent scattering between the two dispersion branches, delocalizing the trion's electron and reducing the trion binding energy.

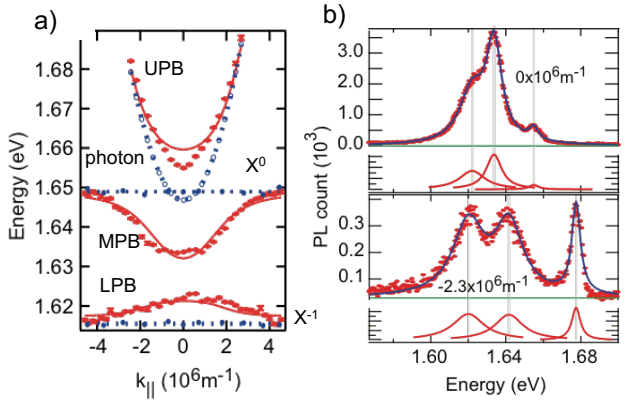

Figure 3. Microcavity polaritons with $MoSe_2$. a) Angle resolved photoluminescence spectrum from the sample as illustrated in Fig. 5a. **b)** The extracted transition energies from the data in Fig. 7a. Clear are polariton branches resulting from the hybridization of the cavity photon, $MoSe_2$ neutral exciton and trion. Data taken at 4K.

The proposed program has three main scientific threads that leverage the advances and infrastructure of the previous program to advance the frontier of integrated nanophotonic devices. Two approaches to integrated nanophotonic *photon* lasers based on van der Waals heterostructures are described and then a novel approach to integrated nanophotonic devices that leverage cavity polaritons based on 2D materials is presented. In the latter effort we will explore *polariton lasers* as well as modulators that utilize unique 2D material properties. If the polariton nonlinearities are strong enough, we will also attempt to realize a polariton blockade that can change the statistics of an illuminating coherent state from Poissonian to sub-Poissonian (ie squeezed). All device architectures will be empowered by the large exciton binding energy intrinsic to TMDCs to enable room temperature device operation and will build directly on the previous program AFOSR

FA9550-16-1-0020. We anticipate photon confinement, coupled with unique TMDC exciton physics, should result in compact nanophotonic devices that are able to reduce device power consumption as well potentially operate at speeds approaching 100's of GHz. The various approaches to lasing described below are motivated by the recognition that a laser's threshold - the minimum amount of material excitation that must be injected before laser oscillation can commence –quantifies static device performance, and its dynamic operation.

Valley-lasers with van der Waals heterostuctures: Most modern electronic devices conceptualize the electron charge as the fundamental unit of information. However, it is also possible to build logic devices using other degrees of freedom of the electron. For example, the spin degree of freedom is used for spintronic devices [33]. Surprisingly, in certain materials, as described below, electrons and holes (as well as excitons), can inherit a binary degree of freedom that is determined by their crystal momentum. This so-called valley degree of freedom has recently attracted great interest as a potential information carrier and led to multiple proposals for valley based optoelectronic devices. One scenario where the valley index is relevant is in materials whose conduction and valence band edges occur at two inequivalent, but energy degenerate points (the K, -K points) of the Brillouin zone. This is illustrated in Fig. 7. The two-inequivalent "K" points can be thought as bits in information processing and give rise to the concept of valleytronics [34].

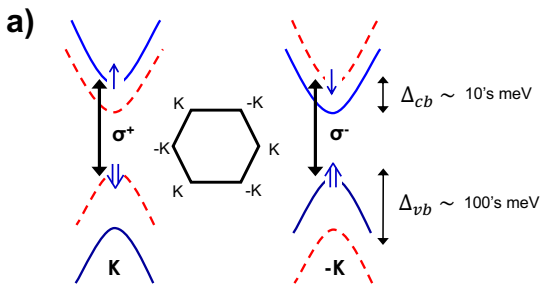

Figure 7. The valley degree of freedom. a) Inset: 2D material first Brillouin zone. The low energy physics at the K and -K points (the valley degree of freedom). Right (left) hand circularly polarized photons σ^+ (σ^-) drive transitions at the K (-K) point. Spin-orbit coupling breaks conduction and valence band degeneracy locking the spin and valley index. Single (double) arrows represent the electron (hole).

TMDCs provide an ideal platform for exploring the valley pseudospin degrees of freedom. In monolayers, the metal and chalcogen atoms form a 2D hexagonal lattice that lacks spatial inversion symmetry. The breaking of inversion symmetry and the spin-orbit interaction produces valley contrasting physical quantities and optical selection rules at the conduction and valence band edges located at ±K points in momentum space (see Fig. 7). This is unlike bilayer TMDCs and graphene where both are centrosymmetric. Further, the conduction and valence band edges are at the ±K points are formed predominantly by the partially filled d-orbitals of the heavy metal atoms in TMDC monolayers that lead to strong spin-orbit coupling. This lifts the energy degeneracy of the spin states in the valence bands in the ±K valley by 100's of mev (Δ_{vb}). The conduction band also has a small but finite spin-valley splitting (Δ_{cb}) with a magnitude of few tens of meV for different monolayers TMDCs. An important consequence of this spin-orbit coupling is that the spin-index becomes locked to the valley index at the band edge. This is illustrated in Fig. 7. Consequently, spin can be selectively excited through valley optical selection rule and intervalley scattering is suppressed due to a large k space separation between the two valleys. Further, the spin-split valence bands at the individual K (-K) valleys affords protection from both the spin and valley flips, as a result, long lifetime of valley polarization is expected. This valley contrast can be exploited to produce a valley Hall effect (carriers in different valleys flow to opposite transverse edges on application of an in-plane electric field) as well as allowing for the optical preparation, control, and detection of valley pseudospin polarization. Therefore, information may be readily

encoded not only by the spin up or down states of an electron (or hole), but also by the two momentum indices whether it resides in the K or -K valley.

Building on our previous results, we have recently fabricated devices that support ***room temperature cavity polaritons*** that utilize WSe_2 neutral excitons as a platform for ***valley polaritonics***. This data is unpublished. Figure 4 presents initial spectroscopic characterization of the device. The monolithic DBR cavity is comprised of two SiO_2/Si_3N_4 (n=1.5 and n=2.0) mirrors and a SiO_2 cavity layer that contains a single flake of WSe_2 at the cavity anti-node. The observed cavity reflectance, see Fig. 4b, has a resonance commensurate with the WSe_2 neutral exciton; see Fig. 4c for measured photoluminescence. Relying on the instrument described in Fig. 2, we have been able to measure the full room-temperature polariton dispersion curve. Cavity polariton data is presented in Fig 8d and exhibits a Rabi splitting of ~ 20 meV. With this device we are able to access the polariton valley degree of freedom, observe cavity-polariton valley polarization and, for the first time, observe valley polariton coherence.

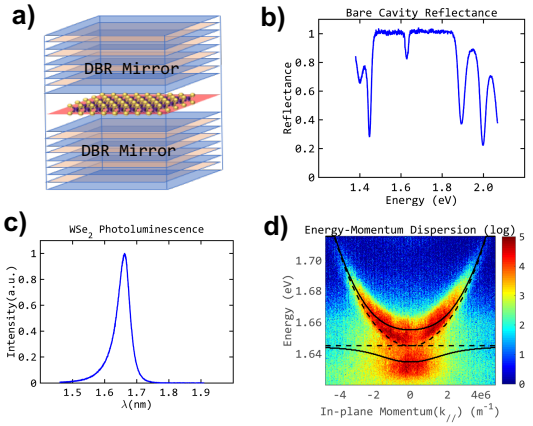

Figure 4. Room temperature cavity polaritonics. a) The fabricated device. It is a monolithic DBR cavity comprised of SiO_2/Si_3N_4 (n=1.5 and n=2.0) mirrors and a SiO_2 cavity layer that contains a single flake of WSe_2 at the cavity anti-node. b) Cavity reflectance. c) Room temperature WSe_2 photoluminescence. d) Observation of room temperature cavity polariton formation. Dispersion measured with instrument in Fig. 5. All data is

To assess the degree of room temperature valley-polariton polarization and coherence, we relied on polarization resolved photoluminescence. In the first set of measurements, a right hand circularly polarized (σ^+) laser excites electron-hole pairs selectively in the K-valley, which then form valley polarized excitons. As seen in Fig. 5a, stronger emission is observed in the co- polarized spectra than the cross polarized spectra, indicating that, indeed, the photo-excited carriers preferentially formed valley-polaritons in the valley they were excited in creating a valley polarization. The observed degree of valley polarization is sensitive to the exact energy of valley-polariton creation. As presented in Fig. 5b, as the pump energy moves closer to the lower polariton branch (see Fig. 4d) the degree of valley polarization is enhanced. This is attributed to less opportunity to intervalley scatter prior to lowest energy valley-polariton formation and optical recombination. Based on the previous observation, although not presented, we are also beginning to explore ***valley-trion-polaritons*** based on our earlier device. We anticipate the reduced intervalley trion scattering, it requires an additional spin to flip, will lead to enhanced ***valley-trion-polariton polarization***.

The creation and detection of valley coherence is another manifestation of valley optical selection rules and coherence creation is critical to utilize the valley degree of freedom as a quantum information bearing entity. A coherent superposition of a left and right circularly polarized laser excitation, i.e., a linearly polarized photon can transfer optical coherence into valley-polariton

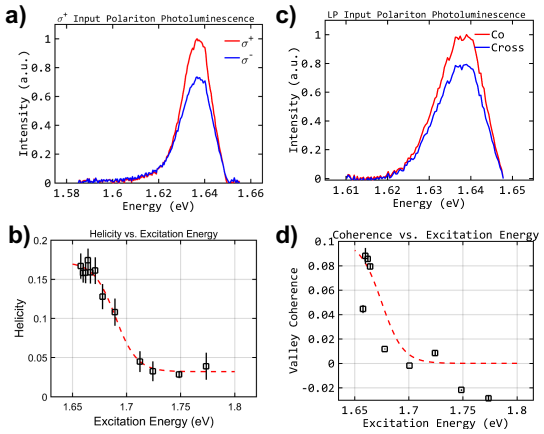

Figure 5. Room temperature valleypolaritonics. a) Observed K-valley polariton valley polarization. Circular polarization contrast reveals valley-polariton polarization. b) Pump energy dependence of valley polariton polarization. Excitation closer to the polariton resonance enhances valley polariztaoin due to reduced scattering c) Observed valley polariton valley coherence. Linear polarization contrast reveals valley-polariton coherence. d) Pump energy dependence of valley polariton cohernece. Excitation closer to the polariton resonance enhances valley coherence due to reduced scattering. All this presented data, from the PIs lab, is unpublished.

coherence. Specifically, the pump laser creates a *coherent superposition of K and -K valley-polaritons*. As seen in Fig. 5c, stronger emission is observed in the co-polarized spectra than the cross polarized spectra, indicating that, indeed, the laser coherence was transferred to a valley-polariton coherence. Thus, the optically generated valley coherence survives the exciton formation and recombination processes, suggesting a long valley dephasing time**.** Similar to the valley-polariton polarization, the valley-polariton coherence is enhanced the closer the pump laser is to the lower polariton resonance (see Fig 5d.).

Polariton lasing: In contrast to photon lasers , the motivation for this effort is to utilize the strongly coupled 2D excitons and cavity photons to demonstrate new regimes of lasing. As a first step towards observing signatures of condensation, we have explored the emitted photon irradiance when pumping the system resonantly into the middle polariton branch of the device described in the section *State-of-the-art in 2D material polariton physics* (see MPB of Fig. 1a). We observed different nonlinear increase of the PL intensity in the LPB and MPB near $k_{\parallel} = 0$. Figure 6a and 6b shows the result of our experiment; note that the power dependence of the measured irradiance changes at different pump energy. The trion-polariton shows a saturation at every pump energy except around 742 nm (1.67 eV) where it has a nonlinear "S" shape in the log-log scale which resembles the power dependence seen in previous reports of polariton lasing from a condensate. At the same pump energy, the exciton polariton also has a "S" shape but not as prominent as the trion-polariton. In addition, we observe that the saturation threshold of the exciton polariton increases as we go deeper into the middle polariton branch. All of these are potential signatures of condensation, but require further experiments to completely demonstrate, for the first-time, cavity polariton lasing based on 2D materials.

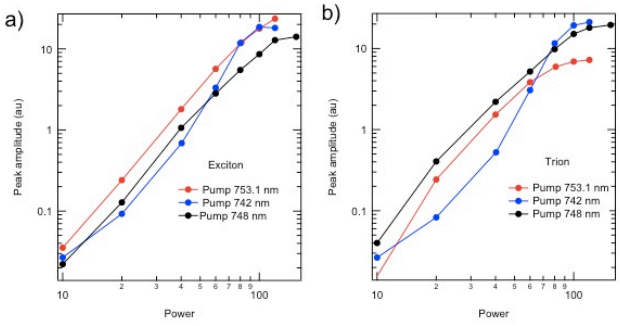

Figure 6. Toward polariton condensation. **a)** Flux emitted from the MPB at $k_{\parallel} = 0$ for three different excitation energies as a function of excitation power. **b)** Same as **a)** but for LPB.